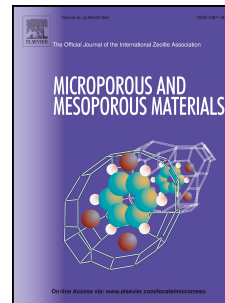


Accepted Manuscript

Sol-gel synthesis of SBA-15: Impact of HCl on surface chemistry

Cyril Pirez, Jean-Charles Morin, Jinesh C. Manayil, Adam F. Lee, Karen Wilson



PII: S1387-1811(18)30302-0

DOI: [10.1016/j.micromeso.2018.05.043](https://doi.org/10.1016/j.micromeso.2018.05.043)

Reference: MICMAT 8945

To appear in: *Microporous and Mesoporous Materials*

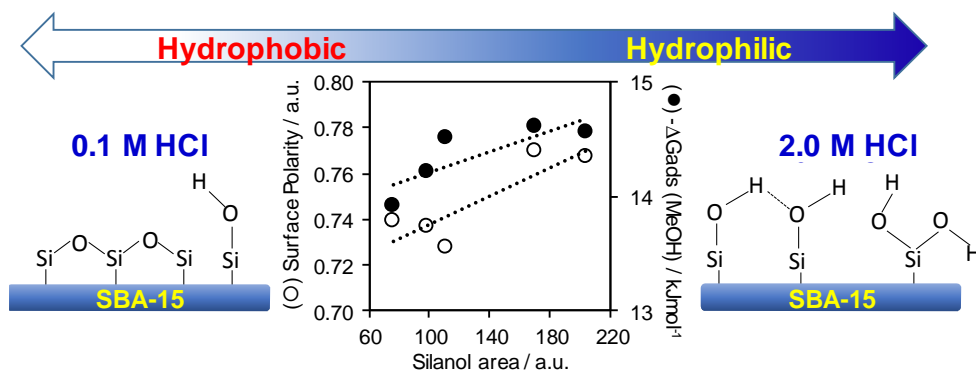
Received Date: 21 February 2018

Revised Date: 18 May 2018

Accepted Date: 28 May 2018

Please cite this article as: C. Pirez, J.-C. Morin, J.C. Manayil, A.F. Lee, K. Wilson, Sol-gel synthesis of SBA-15: Impact of HCl on surface chemistry, *Microporous and Mesoporous Materials* (2018), doi: 10.1016/j.micromeso.2018.05.043.

This is a PDF file of an unedited manuscript that has been accepted for publication. As a service to our customers we are providing this early version of the manuscript. The manuscript will undergo copyediting, typesetting, and review of the resulting proof before it is published in its final form. Please note that during the production process errors may be discovered which could affect the content, and all legal disclaimers that apply to the journal pertain.



Sol-gel synthesis of SBA-15: impact of HCl on surface chemistry

Cyril Pirez^{*a}, Jean-Charles Morin^a, Jinesh C. Manayil^b, Adam F. Lee,^c and Karen Wilson^{*c}

^aUCSS, Université de Lille Nord de France, Lille, France

^bEuropean Bioenergy Research Institute, Aston University, Birmingham, B4 7ET, UK

^cSchool of Science, RMIT University, Melbourne, Vic 3001, Australia

***Corresponding Authors:** karen.wilson2@rmit.edu.au; cyril.pirez@gmail.com

Keywords: SBA-15; hydrothermal synthesis; silanol density; surface energy; Inverse gas chromatography (IGC)

Abstract:

Surface functionalisation of mesoporous silicas is critical to their application as sorbents and catalyst supports. Here we report the impact of chloride on the physicochemical properties of SBA-15, notably the surface density of reactive hydroxyl groups. Bulk and surface properties were characterised by N₂ porosimetry, X-ray diffraction, SEM, TEM, FTIR spectroscopy, and Inverse gas chromatography (IGC). Increasing the HCl concentration from 0.1→2.0 M during the sol-gel preparation of SBA-15 increased the surface silanol coverage two-fold, and slightly widened mesopores from 4.2 to 4.9 nm. IGC reveals that the specific surface energy and corresponding surface polarity of SBA-15 correlate with surface silanol properties, and hence tuning the HCl concentration during SBA-15 synthesis offers a facile route to hydrophilic or hydrophobic silicas, and in turn a means to control their functionalisation and sorptive properties.

1. Introduction

Since the discovery of mesostructured templated silicas by the Mobil Oil Corporation in 1992 [1] they have found application in catalysis,[2] drug delivery and release,[3] adsorption and separation science, and liquid chromatography.[4-6] Such templated porous materials offer ordered pore networks and high surface areas which afford high loadings of uniformly dispersed active sites for catalysis or adsorption/separation applications, rendering them superior to conventional supports possessing disordered pore networks. Since the report of MCM,[1] other silica-derived materials have been discovered such as HMS,[7] KIT-6[8] and SBA-15.[9, 10] The latter is attractive as a catalyst support since the associated Pluronic templates facilitate large average pore diameters (5-15 nm),[11] thick walls and excellent structural stability.[12] Organic modification of SBA-15 via post synthesis grafting (silylation) with alkyoxysilanes is a popular method to incorporate functional groups such as amines,[13, 14] nitriles,[15] carboxylic acids,[15] thiols,[13] and sulfonic acids[16] for catalysis or adsorption applications. The broad appeal of such surface modification processes is evident from the wide range of associated literature, with incorporation of acidic moieties explored for a range of reactions including esterification, transesterification, and dehydration,[17],[18] basic moieties exploited for CO₂ adsorption[19] and condensation reactions,[20] and chelating agents such as carboxylic acid, thiol, or amine groups showing promise for heavy metal adsorption[21] and enzyme immobilisation.[15] However, post-grafting methods are limited by the low surface silanol loadings (essential for functional group attachment) intrinsic to conventional SBA-15.[22]

The nature and distribution of silanol groups on silica surfaces are highly sensitive to the synthetic route. Infra-red studies on amorphous silica identify the presence of isolated and geminal silanols at 3700-3750 cm⁻¹, weakly interacting vicinal pairs at 3500 cm⁻¹,[23] and perturbed silanols at 3650 cm⁻¹ (which are identified as non-accessible being located within intergrain voids).[24]

While the surface of mesoporous materials such as MCM-41 is composed of similar isolated, geminal and vicinal pairs of silanol groups,[25] SBA-15 exhibits another wide band at 3200-3500 cm^{-1} attributed to vicinal chains, which are less reactive towards grafting due to a strong interaction with neighbouring silanols. Identifying the location of particular silanol classes on silica surfaces is difficult, however it is suggested that SBA-15 possesses a high concentration (~70 %) of silanol groups within the micropores produced by conventional sol-gel and hydrothermal syntheses, which may be inaccessible to even small silanes.[26]

Organosilane grafting on pre-formed silica surfaces is typically performed using either chloroform[27],[28], toluene,[16] or $\text{H}_2\text{O}/\text{NaCl}$ mixtures[18] as a solvent. Methods using organic solvents under anhydrous conditions are believed to favour preferential grafting of the isolated silanol groups prevalent on more hydrophobic silica surfaces.[29] However, the use of $\text{H}_2\text{O}/\text{NaCl}$ mixtures in hydrothermal saline promoted grafting (HSPG) treatments, can activate hydrophobic and hydrophilic silica surfaces, delivering higher loadings of grafted groups; it is believed that Cl^- influences the silanol distribution by disrupting (surface) hydrogen bonded networks.[18]

Anion addition during the synthesis of templated silica materials is usually motivated by their role in aiding micelle formation through decreasing the solubility of organic solutes in water. Such anions can be classified according to the so-called 'Hofmeister series' according to their ability to shift the phase equilibrium at a given molar concentration and follows: $\text{SO}_4^{2-} = \text{HPO}_4^{2-} > \text{F}^- > \text{Cl}^- > \text{Br}^- > \text{I}^- > \text{SCN}^-$. Anions to the left-hand side of the Hofmeister series are believed to be 'structure-makers', while those on the right-hand side are 'structure-breakers'. Micellisation and phase separation thermodynamics are perturbed by the increased ionic strength following salt addition, with smaller halides having a higher heat of solvation in water,[30] thereby lowering the CMT (critical micellisation temperature) and CP (cloud point) of aqueous PEO-PPO-PEO solutions. Such effects

have been exploited for acid-free, sol-gel routes to 2D hexagonally-ordered SBA-15 materials, in which alcoholic NaCl is added to Pluronic P123 templating solutions.[31] Halides also offer a means to control the formation kinetics and domain size of silica mesostructures,[32] with NH_4F /decane addition affording porous materials with a highly ordered, cuboid-like morphology: in this example, disordered mesoporous silicas formed in the absence of NH_4F . [33]

SBA-15 is conventionally synthesised in the presence of HCl, and while only a handful of studies have investigated the influence of HCl concentration on the morphology of sol-gel synthesised SBA-15,[32, 34] none have explored its impact on surface hydroxylation and surface energetics. Here we explore the latter effect, through varying the concentration of HCl employed during the sol-gel synthesis of a SBA-15 mesoporous silica. Silanol densities were proportional to [HCl] during sol-gel synthesis, and favoured by shorter gelation periods. Increased silanol densities correlate with enhanced surface polarity.

2. Experimental

2.1. Preparation of SBA-15 with different HCl concentrations

Briefly, 2.4 g of Pluronic P123 triblock copolymer was dissolved in 84 ml of aqueous HCl of chosen concentration (2, 1.5, 1, 0.5, or 0.1 M), and stirred at 35 °C for 72 h. Subsequently 5.5 ml of tetraethoxyorthosilicate (TEOS, 98 %, Acros Organics) was added to the solution which was maintained at 35 °C for a further 72 h gelation period under stirring (to ensure full hydrolysis and condensation of TEOS even at low [HCl]). A conventional SBA-15 reference was also prepared using 2 M HCl and a 24 h gelation period. The resulting sol-gel slurries were hydrothermally aged at 80 °C for 24 h, after which the solid product was filtered, washed 3 times with deionised water, and

calcined in static air at 550 °C for 6 h (ramp rate 5 °C.min⁻¹). These materials are denoted xSBA-15 where x = 2.0, 1.5, 1.0, 0.5, or 0.1 M, with the reference denoted 2.0SBA-15-24h.

2.3. Characterisation

Surface areas and BJH pore size distributions were determined by N₂ porosimetry using a Quantachrome Nova 2000e porosimeter, with isotherms processed using NOVWin software. Samples were degassed at 120 °C for 2 h before analysis by N₂ adsorption at -196 °C. BET surface areas were calculated over the relative pressure range 0.01-0.2, while pore diameters and volumes were calculated by applying the BJH method to the desorption isotherm for relative pressures >0.35. Low-angle powder XRD patterns were recorded on a PANalytical X'pertPro diffractometer fitted with an X'celerator detector and Cu K_α (1.54 Å) source with the goniometer calibrated against a Si standard (PANalytical). Low-angle patterns were recorded over the range 2θ = 0.3-8 ° with a step size of 0.01 °. TEM was performed using a JEOL 2100 transmission electron microscope operated at 200 kV, with images recorded by a Gatan Ultrascan 1000XP digital camera, and image analysis undertaken using ImageJ software. Transmission IR measurements were recorded with a Nicolet Protege System 460 equipped with a MCT detector, using self-supporting wafers (5 mg.cm⁻²) prepared from uniformly-ground samples. Samples were placed in a transmission cell and heated at 200 °C under high vacuum (10⁻⁶ mbar) for 2 hr prior to spectral acquisition, sufficient to remove any contribution from physisorbed water to the silanol region.[35] DRIFTS measurements were conducted using a Thermo Scientific Nicolet environmental cell and smart collector accessory on a Thermo Scientific Nicolet iS50 FT-IR Spectrometer with MCT detector. The catalysts diluted in KBr (10 wt%) were loaded in the environmental cell and evacuated at 200 °C for 2 h to remove physisorbed water/moisture. Analyses were performed at 200 °C, with final spectra normalised to

the band at 1850 cm^{-1} characteristic Si-O-Si vibrations of SBA-15.

Surface energies at infinite dilution were determined by a fully-automated Inverse GC system (IGC) (Surface Measurement Systems Ltd), following our previously reported method.[36, 37] Briefly samples were outgassed for 2 h at $120\text{ }^{\circ}\text{C}$ to remove physisorbed water and impurities, after which they were exposed to pulses of polar (dichloromethane, acetonitrile, ethyl acetate, methanol) and apolar (hexane, heptane, octane, nonane, and decane) probe molecules. Dispersive surface energies were calculated from the gradient of a plot of $RT\ln V_N$ versus $\alpha(\gamma_L^D)^{\frac{1}{2}}$ (equation 1):

$$RT\ln V_N = 2N_A(\gamma_S^D)^{\frac{1}{2}}\alpha(\gamma_L^D)^{\frac{1}{2}} + \text{constant} \quad (1)$$

where N_A is Avogadro's number, α is the surface area occupied by the probe molecule, V_N is the specific retention volume and γ_S^D and γ_L^D are dispersive components of the solid and liquid surface energy respectively. Specific surface energies are calculated from the deviation of $RT\ln V_N$ values for polar probes and the gradient of the plot of $RT\ln V_N$ versus $\alpha(\gamma_L^D)^{\frac{1}{2}}$.

3. Results

3.1 Effect of [HCl] on textural properties

The successful synthesis of a family of xSBA-15 materials, employing 0.1-2 M HCl and a gelation period of 72 h, was first verified by N_2 porosimetry and XRD. N_2 porosimetry (**Fig. S1**) confirmed all materials exhibit Type IV isotherms with H1 hysteresis loops characteristic of SBA-15. The isotherm hysteresis loop shifted slightly to higher partial pressure with increased [HCl], while BJH pore size distributions revealed a monotonic increase in the average pore diameter from 4.2→4.9 nm (**Fig. 1**). All materials exhibit well-defined low-angle reflections (**Fig. 2**) corresponding to the 100,

110 and 200 planes characteristic of the p_{6mm} hexagonal structure of SBA-15,[10] confirming that structural integrity and long range order was retained with increasing [HCl]. The hydrodynamic diameter of P123 micelles in water is reported to increase with [HCl] due to stronger hydrogen bonding with protonated water molecules and expansion of the outer PEO micellar corona.[38, 39] In the presence of TEOS, high [HCl] are proposed to increase the density of silicatropic liquid-crystal seeds arising from acid catalysed hydrolysis of the silane, and passivate their growth, resulting in thinner walls. [40] The net result is an increase in pore diameter, but constant unit cell size.

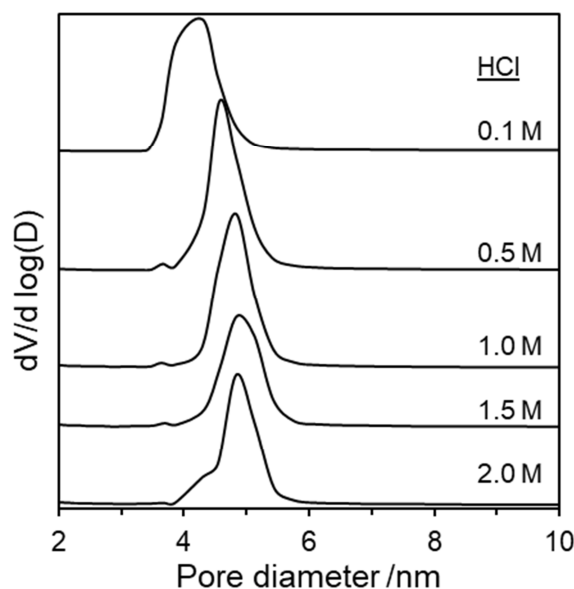


Fig. 1. BJH pore size distribution of SBA-15 prepared with varying [HCl] (offset for clarity).

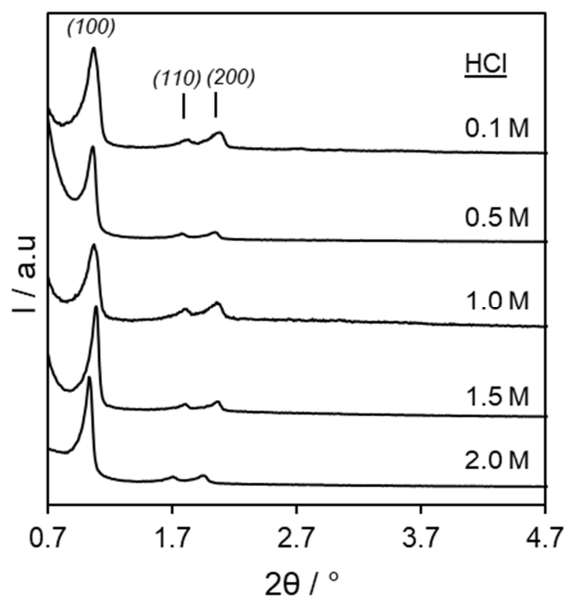


Fig. 2. Low-angle XRD patterns of SBA-15 prepared with varying [HCl] (offset for clarity).

Comparison of N₂ porosimetry data with the 2.0SBA-15-24h reference material (**Fig. S2**) shows that the hysteresis loop of the desorption isotherm shifted to higher partial pressure upon decreasing the gelation time from 72→24 h, associated with an increase in the average mesopore diameter (**Fig. S3a**) and consistent with a shift of low-angle XRD reflections to lower angle (**Fig S3b**). Such observations are in accordance with literature, wherein silicate assembly is reported to occur rapidly around the Pluronic template during the first two hours of SBA-15 synthesis,[41] and followed by micelle contraction and elongation during densification of the walls; [42] gelation times up to 24 h result in decreased pore diameters.[43] Longer gelation times are not reported in the literature, however our present results suggest that the evolution of structural properties continues. Textural and structural properties of the different SBA-15 materials are summarised in **Table 1**, which shows that 2.0SBA-15 exhibited a higher specific area and pore volume for shorter aging times (24 h)

ACCEPTED MANUSCRIPT

Table 1. Textural and structural properties of SBA-15 prepared with 0.1-2.0 M [HCl] and 72 h gelation time. Conventional SBA-15 prepared at 2 M [HCl] and 24 h gelation time shown for reference.

Materials	BET ^a	Vp	BJH pore	Plane	Unit cell	Wall
	/m ² g ⁻¹	/cm ³ ·g ⁻¹	diameter ^b	spacing ^c	parameter ^d	thickness ^e
			/nm	/nm	/nm	/nm
0.1SBA-15	611	0.63	4.2	8.1	9.4	5.1
0.5SBA-15	766	0.74	4.7	8.2	9.5	4.8
1.0SBA-15	845	0.90	4.9	8.3	9.6	4.7
1.5SBA-15	873	0.80	4.9	8.2	9.5	4.6
2.0SBA-15	928	0.87	4.9	8.1	9.4	4.6
2.0SBA-15-24h	1130	1.2	5.4	8.6	9.9	4.5

^aFrom BET equation. ^bAnalyzed from the desorption branch. ^cFrom Bragg's law assuming that the peak corresponds to the (100) plane. ^d $a_0 = (2d_{100})/\sqrt{3}$. ^e a_0 - pore diameter.

SEM micrographs demonstrate that increasing the acid concentration between 0.1 and 1.5 M HCl has little impact on the size or morphology of SBA-15, which forms extended worm-like fibrous bundles (**Fig. 3**). However, high concentrations of HCl are known to increase the rate of silica condensation and hence favour lower aspect ratio nanostructures, consistent with the transition from a fibre to particulate morphology observed for the 2.0SBA-15 sample.[9] TEM (**Fig. 4**) confirmed preservation of the 2D hexagonal structure for all the SBA-15 materials, irrespective of [HCl] or gelation time.

ACCEPTED MANUSCRIPT

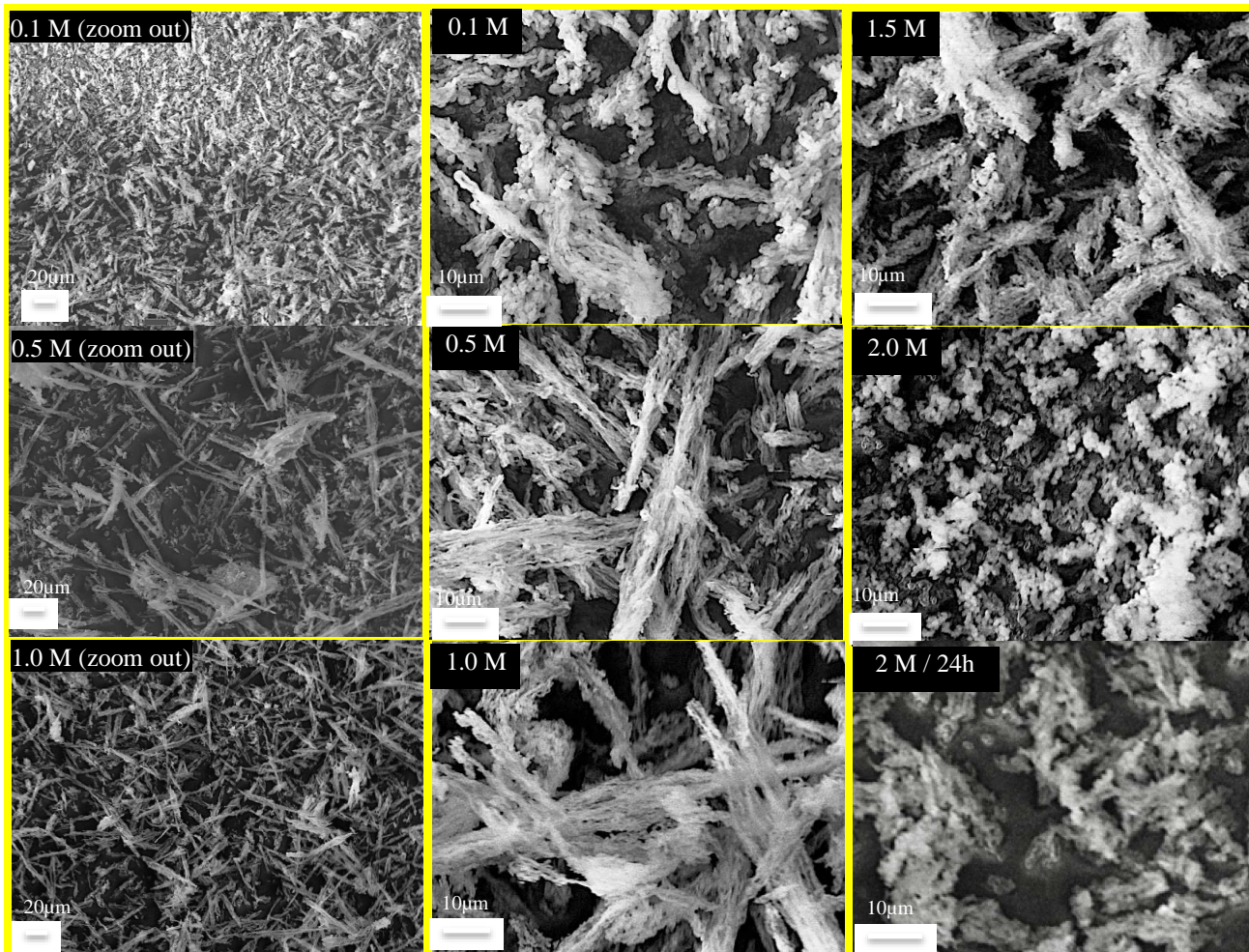


Fig. 3: SEM of xSBA-15 prepared with 0.1-2.0 M HCl and 72 h gelation; conventional 2.0SBA-15-24h shown bottom right for comparison.

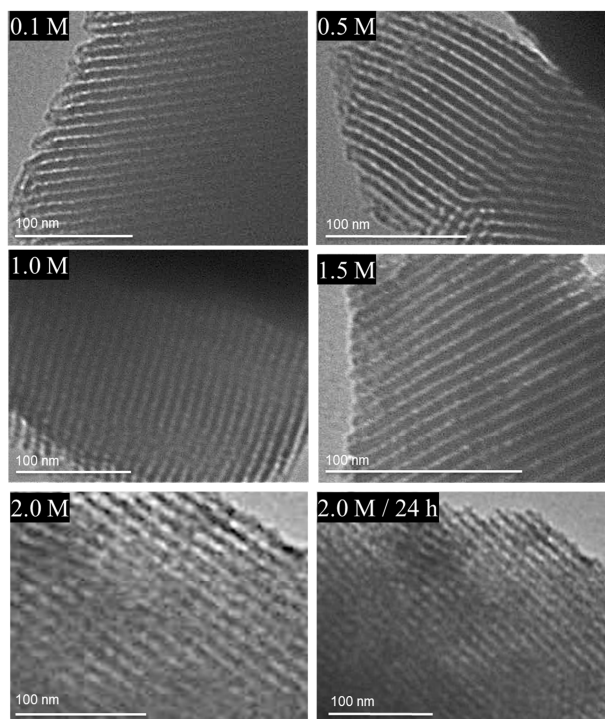


Fig. 4: TEM of xSBA-15 prepared with 0.1-2.0 M HCl and 72 h gelation; conventional 2.0SBA-15-24h shown bottom right for comparison.

Transmission FTIR spectra were subsequently recorded to assess the effect of [HCl] and gelation time on the surface hydroxyl content of SBA-15. **Fig. 5** shows that all materials exhibited vibrational modes over the range 3200-3800 cm^{-1} characteristic of isolated, germinal, and vicinal silanols as depicted in **Scheme 1**. The band at 3710-3750 cm^{-1} is assigned to the stretching mode of either terminal silanols in a hydrogen-bonded vicinal chain, isolated silanols, or geminal silanols that lack hydrogen-bonded neighbours, while the broad band at 3000-3550 cm^{-1} is assigned to H-bonded silanols in vicinal chains.[29] Note that solid state ^1H and ^{29}Si NMR studies demonstrate that vicinal silanols are stable at the surface of porous silicas and aluminosilicates even after high temperature calcination at between 550 and 600 $^\circ\text{C}$. [26, 44, 45] Clustering of silanol groups on SBA-15 gives rise to surface regions having different polarity: hydrophobic regions where siloxane bridges are located alongside isolated and geminal silanols ($>3730 \text{ cm}^{-1}$), and hydrophilic regions dominated by vicinal

groups ($<3730\text{ cm}^{-1}$). According to Cauvel and co-workers,[46] the local environment of isolated silanols further modulates their acidity and stretching frequency.

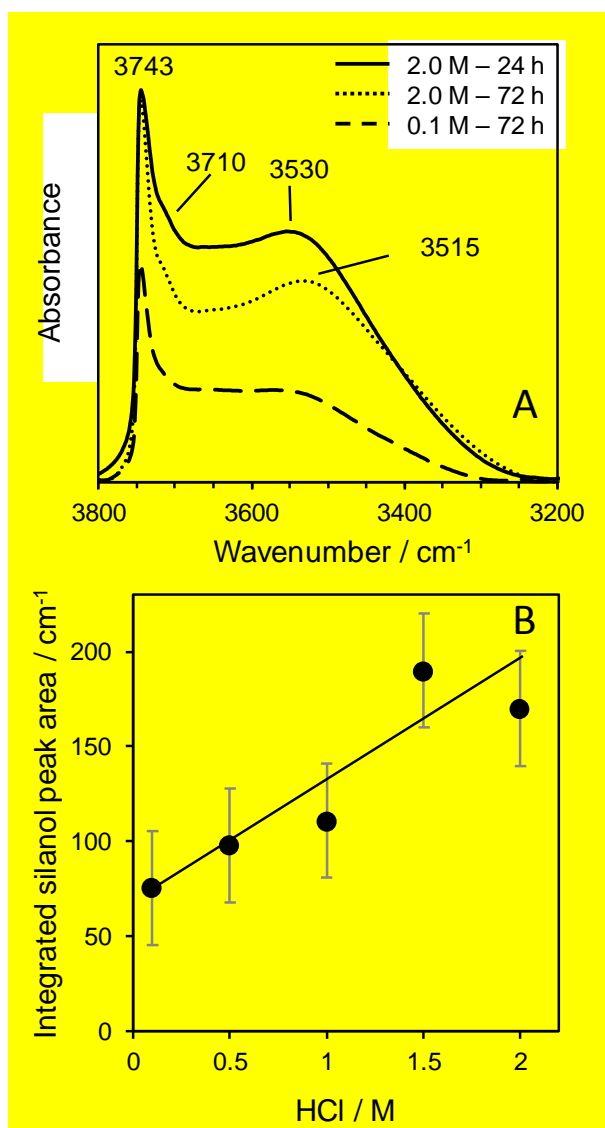
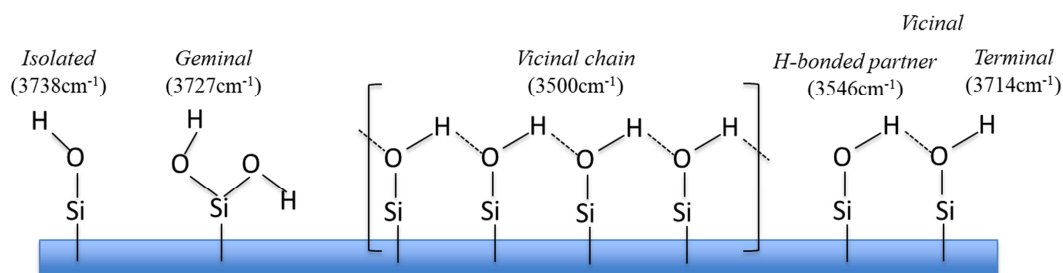


Fig. 5. Transmission FTIR spectra of SBA-15 as a function of [HCl] and gelation time: a) representative spectra of silanol region for 0.1 and 2.0 M [HCl] after 72 h gelation, alongside 2.0SBA-15-24h reference for comparison (spectra are normalised to the band at 1850 cm^{-1} characteristic of Si-O-Si vibrations); b) total silanol peak area from normalised spectra as function of [HCl] for xSBA-15.



Scheme 1: Typical frequencies of silanol groups on silica surfaces

H-bonded silanols typically have a longer average O-H bond than isolated silanols, leading to lower vibrational frequencies in the order isolated (non-H bonded) > proton donor > proton donor-acceptor. Hence, the sharp band at 3743 cm^{-1} in **Fig. 5a** is assigned to isolated and geminal silanols, while the shoulder at 3710 cm^{-1} is assigned to terminal silanol groups with a H-bonded partner. **Fig. 5a** shows that for SBA-15 prepared using 2 M HCl, the gelation time strongly influences the distribution of isolated, geminal, and vicinal silanols, with 24 h aged samples exhibiting a high density of vicinal silanols, whereas 72 h ageing favours isolated, geminal, and terminal silanols at the expense of vicinal silanols. Increasing the gelation time in acidic media promotes condensation of vicinal silanols, breaking up their domains and redistributing more hydrophobic silanol species. These observations are consistent with Si^{29} MAS-NMR studies which reveal an increased contribution from Q^4 species on increasing gelation time from 2→24 h, attributed to silanol condensation.[43] Increased crosslinking of silanols under acidic conditions is also expected to densify silica walls, resulting in narrower pore diameters and increased wall thickness,[12] consistent with our results in **Table 1**.

Varying the [HCl] provides further insight into the silanol cross-linking process during SBA-15 synthesis, and a potential role of the Cl^- anion in influencing the -OH distribution or stability. **Fig. 5b** shows that the overall intensity of silanol modes is directly proportional to [HCl], a surprising

observation since the concomitant increase in acidity would be expected to favour condensation reactions. This observation suggests that surface Cl^- inhibits cross-linking of adjacent silanols, thereby helping to stabilise vicinal chains, particularly at short gelation times (≤ 24 h). DRIFT spectra (**Fig. S4**) of the Si-O-Si vibrational modes over the range $960\text{-}1450\text{ cm}^{-1}$ evidence little sensitivity of the local silica framework to $[\text{HCl}]$. These spectra are characterised by siloxane modes, which fall in two broad bands. The first, spanning $960\text{-}1110\text{ cm}^{-1}$, is assigned to $\nu(\text{Si-OH})$, $\nu_{\text{as}}(\text{Si-O-Si})$ modes of cyclic structures, and the transverse TO_3 $\nu_{\text{as}}(\text{Si-O-Si})$ mode of 6-ring structures. The second, spanning $1110\text{-}1250\text{ cm}^{-1}$ is assigned to the $\nu_{\text{as}}(\text{Si-O-Si})$ mode of linear chains (associated with Si-OH groups[47]), and the $\nu_{\text{as}}(\text{Si-O-Si})$ and longitudinal LO_3 $\nu_{\text{as}}(\text{Si-O-Si})$ modes of 6-ring structures [48, 49].

3.3 Effect of $[\text{HCl}]$ on surface energetics:

The redistribution of surface silanols between isolated silanols and (hydrophobic) siloxane bridges and (hydrophilic) geminal and H-bonded vicinal silanol groups or vicinal chains are expected to perturb the corresponding surface energy and polarity. The latter properties are amenable to quantification by inverse gas chromatography (IGC), a powerful tool for probing the surface chemistry of porous materials.[36] Specific (polar) and non-specific (dispersive) interactions of polar and non-polar molecules can be correlated with surface hydrophilicity, while the interaction of non-polar molecules (alkanes) with surfaces via weak London forces correlates with surface hydrophobicity. IGC can be thus be used to elucidate changes in the distribution of hydrophobic siloxane and hydrophilic silanol groups on SBA-15 surfaces according to the surface polarity, X_p , defined as the ratio of the specific (hydrogen bonding) surface energy to the total surface energy [50] (Equation 2).

$$Xp = \frac{\gamma_S^{SP}}{(\gamma_S^{SP} + \gamma_S^D)} \quad (2)$$

Fig. 6 and **Table 2** shows that both Xp , and free energy of methanol adsorption of a prototypical polar probe molecule, $-\Delta G_{\text{ads}}(\text{MeOH})$, of our xSBA-15 materials is directly proportional to the total silanol group loading determined from transmission FTIR (**Fig. 5**). This relationship accords with chemical intuition that increasing the surface coverage of geminal and H-bonded vicinal silanols should increase the polarity of silica, and provides a semi-quantitative scale by which the surface polarity of SBA-15 can be tuned to control subsequent functionalisation and/or adsorption/catalysis through shifting reaction equilibria [37, 51].

Table 2: Integrated silanol peak areas from FTIR for sol-gel SBA-15 at different [HCl], and corresponding data from IGC surface energy analysis.

[HCl] used in SBA-15 synthesis	Silanol area / a.u	Dispersive surface energy (γ_S^D) /mJ.m ⁻²	Specific surface energy (γ_s^p) /mJ.m ⁻²	Surface polarity	$-\Delta G_{\text{ads}}$ methanol (kJ/Mol)
0.1 M	75.6	80	227	0.74	13.9
0.5 M	98.2	84	235	0.74	14.2
1.0 M	110.9	88	235	0.73	14.5
1.5 M	168.0	78	252	0.76	14.5
2.0 M	170.1	78	261	0.77	14.6
2.0 M – 24 h	203.8	79	260	0.77	14.6

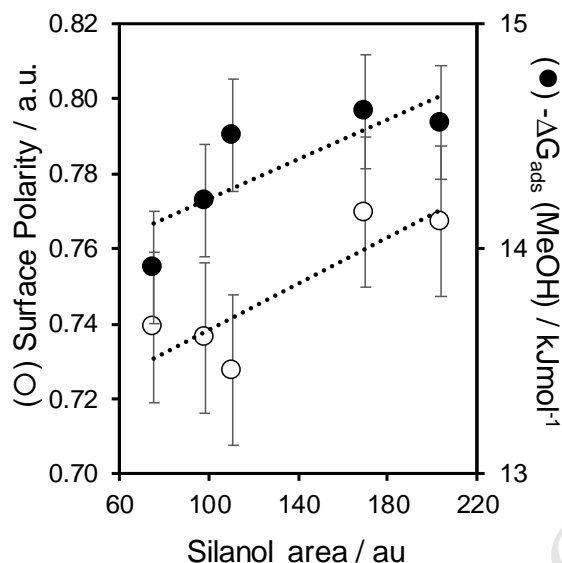


Fig. 6. Correlation between surface silanol loading, surface polarity, and specific free energy of methanol adsorption of xSBA-15 as a function of [HCl].

Conclusions

The impact of chloride anions on the structure and surface properties of SBA-15 has been investigated with the aim of tuning the surface density of reactive hydroxyl groups amenable for subsequent derivatisation. Silanol distributions of SBA-15 materials were controlled by varying the [HCl] and/or gelation time during a conventional sol-gel synthesis. Increasing [HCl] from 0.1-2.0 M resulted in a doubling of the surface silanol coverage, possibly through Cl^- stabilisation of surface silanols and concomitant hindering of silanol cross linking during hydrothermal aging. Longer gelation time under acidic conditions lowered silanol coverages, associated with enhanced crosslinking. Specific surface energies for methanol adsorption and overall surface polarity, measured by IGC, increase with [HCl] mirroring the rise in geminal and H-bonded vicinal surface silanols. The resulting insight offers a simple means to tune the surface hydrophobicity and hydrophilicity of SBA-15, and its subsequent derivatisation for improved catalysts and sorbents.

Acknowledgements

We thank the EPSRC (EP/G007594/2 and EP/F063423/2) for financial support and a Leadership Fellowship (AFL). and the Royal Society for the award of an Industry Fellowship (KW). The authors thank Mr. J.C. Morin for Infrared spectroscopy from Unité de Catalyse et Chimie du Solide. Chevreul Institute (FR 2638).

Declarations of interest none

References

- [1] C.T. Kresge, M.E. Leonowicz, W.J. Roth, J.C. Vartuli, J.S. Beck, Ordered mesoporous molecular sieves synthesized by a liquid-crystal template mechanism, *Nature*, 359 (1992) 710-712.
- [2] A. Corma, From microporous to mesoporous molecular sieve materials and their use in catalysis, *Chemical Reviews*, 97 (1997) 2373-2419.
- [3] I.I. Slowing, J.L. Vivero-Escoto, C.-W. Wu, V.S.Y. Lin, Mesoporous silica nanoparticles as controlled release drug delivery and gene transfection carriers, *Advanced Drug Delivery Reviews*, 60 (2008) 1278-1288.
- [4] L.F. Giraldo, B.L. López, L. Pérez, S. Urrego, L. Sierra, M. Mesa, Mesoporous Silica Applications, *Macromolecular Symposia*, 258 (2007) 129-141.
- [5] P. Makowski, X. Deschanel, A. Grandjean, D. Meyer, G. Toquer, F. Goettmann, Mesoporous materials in the field of nuclear industry: Applications and perspectives, *New Journal of Chemistry*, 36 (2012) 531-541.
- [6] J.Y. Ying, C.P. Mehnert, M.S. Wong, Synthesis and Applications of Supramolecular-Templated Mesoporous Materials, *Angewandte Chemie International Edition*, 38 (1999) 56-77.
- [7] S.A. Bagshaw, E. Prouzet, T.J. Pinnavaia, Templating of Mesoporous Molecular Sieves by Nonionic Polyethylene Oxide Surfactants, *Science*, 269 (1995) 1242-1244.
- [8] T.-W. Kim, F. Kleitz, B. Paul, R. Ryoo, MCM-48-like Large Mesoporous Silicas with Tailored Pore Structure: Facile Synthesis Domain in a Ternary Triblock Copolymer–Butanol–Water System, *Journal of the American Chemical Society*, 127 (2005) 7601-7610.
- [9] D. Zhao, Q. Huo, J. Feng, B.F. Chmelka, G.D. Stucky, Nonionic Triblock and Star Diblock Copolymer and Oligomeric Surfactant Syntheses of Highly Ordered, Hydrothermally Stable, Mesoporous Silica Structures, *Journal of the American Chemical Society*, 120 (1998) 6024-6036.

- [10] D. Zhao, J. Feng, Q. Huo, N. Melosh, G.H. Fredrickson, B.F. Chmelka, G.D. Stucky, Triblock Copolymer Syntheses of Mesoporous Silica with Periodic 50 to 300 Angstrom Pores, *Science*, 279 (1998) 548-552.
- [11] M. Kruk, L. Cao, Pore Size Tailoring in Large-Pore SBA-15 Silica Synthesized in the Presence of Hexane, *Langmuir*, 23 (2007) 7247-7254.
- [12] F. Zhang, Y. Yan, H. Yang, Y. Meng, C. Yu, B. Tu, D. Zhao, Understanding Effect of Wall Structure on the Hydrothermal Stability of Mesostructured Silica SBA-15, *The Journal of Physical Chemistry B*, 109 (2005) 8723-8732.
- [13] A.M. Liu, K. Hidajat, S. Kawi, D.Y. Zhao, A new class of hybrid mesoporous materials with functionalized organic monolayers for selective adsorption of heavy metal ions, *Chemical Communications*, (2000) 1145-1146.
- [14] N. Hiyoshi, K. Yogo, T. Yashima, Adsorption characteristics of carbon dioxide on organically functionalized SBA-15, *Microporous and Mesoporous Materials*, 84 (2005) 357-365.
- [15] H.H.P. Yiu, P.A. Wright, N.P. Botting, Enzyme immobilisation using SBA-15 mesoporous molecular sieves with functionalised surfaces, *Journal of Molecular Catalysis B: Enzymatic*, 15 (2001) 81-92.
- [16] J.P. Dacquin, A.F. Lee, C. Pirez, K. Wilson, Pore-expanded SBA-15 sulfonic acid silicas for biodiesel synthesis, *Chemical Communications*, 48 (2012) 212-214.
- [17] G. Mohammadi Ziarani, N. Lashgari, A. Badieli, Sulfonic acid-functionalized mesoporous silica (SBA-Pr-SO₃H) as solid acid catalyst in organic reactions, *Journal of Molecular Catalysis A: Chemical*, 397 (2015) 166-191.
- [18] C. Pirez, A.F. Lee, J.C. Manayil, C.M.A. Parlett, K. Wilson, Hydrothermal saline promoted grafting: a route to sulfonic acid SBA-15 silica with ultra-high acid site loading for biodiesel synthesis, *Green Chemistry*, 16 (2014) 4506-4509.
- [19] R. Sanz, G. Calleja, A. Arencibia, E.S. Sanz-Pérez, CO₂ Uptake and Adsorption Kinetics of Pore-Expanded SBA-15 Double-Functionalized with Amino Groups, *Energy & Fuels*, 27 (2013) 7637-7644.
- [20] Sujandi, S.-E. Park, D.-S. Han, S.-C. Han, M.-J. Jin, T. Ohsuna, Amino-functionalized SBA-15 type mesoporous silica having nanostructured hexagonal platelet morphology, *Chemical Communications*, (2006) 4131-4133.
- [21] C. Lesaint, F. Frébault, C. Delacôte, B. Lebeau, C. Marichal, A. Walcarius, J. Patarin, Synthesis and characterization of mesoporous silicas functionalized by thiol groups, and application as sorbents for mercury (II), in: S. Abdelhamid, J. Mietek (Eds.) *Studies in Surface Science and Catalysis*, Elsevier2005, pp. 925-932.
- [22] J.A. Melero, R. van Grieken, G. Morales, Advances in the Synthesis and Catalytic Applications of Organosulfonic-Functionalized Mesostructured Materials, *Chemical Reviews*, 106 (2006) 3790-3812.
- [23] B.A. Morrow, Chapter 3 Surface Groups on Oxides, in: J.L.G. Fierro (Ed.) *Studies in Surface Science and Catalysis*, Elsevier1990, pp. A161-A224.
- [24] Y. Wang, B.A. Morrow, Infrared Study of the Chemisorption of Pentamethylantimony on Silica, *Langmuir*, 12 (1996) 4153-4157.
- [25] X.S. Zhao, G.Q. Lu, A.K. Whittaker, G.J. Millar, H.Y. Zhu, Comprehensive Study of Surface Chemistry of MCM-41 Using ²⁹Si CP/MAS NMR, FTIR, Pyridine-TPD, and TGA, *The Journal of Physical Chemistry B*, 101 (1997) 6525-6531.
- [26] M. Ide, M. El-Roz, E. De Canck, A. Vicente, T. Planckaert, T. Bogaerts, I. Van Driessche, F. Lynen, V. Van Speybroeck, F. Thybault-Starzyk, P. Van Der Voort, Quantification of silanol sites

- for the most common mesoporous ordered silicas and organosilicas: total versus accessible silanols, *Physical Chemistry Chemical Physics*, 15 (2013) 642-650.
- [27] P. Dhepe, M. Ohashi, S. Inagaki, M. Ichikawa, A. Fukuoka, Hydrolysis of sugars catalyzed by water-tolerant sulfonated mesoporous silicas, *Catal Lett*, 102 (2005) 163-169.
- [28] G.E.F. X. Feng, L.-Q. Wang, A. Y. Kim, J. Liu, and K. M. Kemner, Functionalized Monolayers on Ordered Mesoporous Supports, *Science*, 276 (1997) 923-926.
- [29] D. Brunel, A. Cauvel, F. Di Renzo, F. Fajula, B. Fubini, B. Onida, E. Garrone, Preferential grafting of alkoxy silane coupling agents on the hydrophobic portion of the surface of micelle-templated silica, *New Journal of Chemistry*, 24 (2000) 807-813.
- [30] P. Alexandridis, J.F. Holzwarth, Differential scanning calorimetry investigation of the effect of salts on aqueous solution properties of an amphiphilic block copolymer (poloxamer), *Langmuir*, 13 (1997) 6074-6081.
- [31] S.-Y. Chen, S. Cheng, Acid-Free Synthesis of Mesoporous Silica Using Triblock Copolymer as Template with the Aid of Salt and Alcohol, *Chemistry of Materials*, 19 (2007) 3041-3051.
- [32] C.V. Teixeira, H. Amenitsch, P. Linton, M. Lindén, V. Alfredsson, The Role Played by Salts in the Formation of SBA-15, an in Situ Small-Angle X-ray Scattering/Diffraction Study, *Langmuir*, 27 (2011) 7121-7131.
- [33] H. Zhang, J. Sun, D. Ma, X. Bao, A. Klein-Hoffmann, G. Weinberg, D. Su, R. Schlögl, Unusual Mesoporous SBA-15 with Parallel Channels Running along the Short Axis, *Journal of the American Chemical Society*, 126 (2004) 7440-7441.
- [34] E.M. Björk, F. Söderlind, M. Odén, Tuning the shape of mesoporous silica particles by alterations in parameter space: from rods to platelets, *Langmuir*, 29 (2013) 13551-13561.
- [35] L. Frattini, M.A. Isaacs, C.M.A. Parlett, K. Wilson, G. Kyriakou, A.F. Lee, Support enhanced α -pinene isomerization over HPW/SBA-15, *Applied Catalysis B: Environmental*, 200 (2017) 10-18.
- [36] C. Pirez, A.F. Lee, C. Jones, K. Wilson, Can surface energy measurements predict the impact of catalyst hydrophobicity upon fatty acid esterification over sulfonic acid functionalised periodic mesoporous organosilicas?, *Catalysis Today*, 234 (2014) 167-173.
- [37] J.C. Manayil, V.C. dos Santos, F.C. Jentoft, M. Granollers Mesa, A.F. Lee, K. Wilson, Octyl Co-grafted PrSO₃H/SBA-15: Tunable Hydrophobic Solid Acid Catalysts for Acetic Acid Esterification, *ChemCatChem*, 9 (2017) 2231-2238.
- [38] B. Yang, C. Guo, S. Chen, J. Ma, J. Wang, X. Liang, L. Zheng, H. Liu, Effect of Acid on the Aggregation of Poly(ethylene oxide)-Poly(propylene oxide)-Poly(ethylene oxide) Block Copolymers, *The Journal of Physical Chemistry B*, 110 (2006) 23068-23074.
- [39] Y. Wan, Y. Shi, D. Zhao, Designed synthesis of mesoporous solids via nonionic-surfactant-templating approach, *Chemical Communications*, (2007) 897-926.
- [40] Y. Wang, F. Zhang, Y. Wang, J. Ren, C. Li, X. Liu, Y. Guo, Y. Guo, G. Lu, Synthesis of length controllable mesoporous SBA-15 rods, *Materials Chemistry and Physics*, 115 (2009) 649-655.
- [41] A.Y. Khodakov, V.L. Zholobenko, M. Impéror-Clerc, D. Durand, Characterization of the Initial Stages of SBA-15 Synthesis by in Situ Time-Resolved Small-Angle X-ray Scattering, *The Journal of Physical Chemistry B*, 109 (2005) 22780-22790.
- [42] E.M. Johansson, M.A. Ballem, J.M. Córdoba, M. Odén, Rapid synthesis of SBA-15 rods with variable lengths, widths, and tunable large pores, *Langmuir*, 27 (2011) 4994-4999.
- [43] T. Benamor, L. Vidal, B. Lebeau, C. Marichal, Influence of synthesis parameters on the physico-chemical characteristics of SBA-15 type ordered mesoporous silica, *Microporous and Mesoporous Materials*, 153 (2012) 100-114.

- [44] M. Hunger, J. Karger, H. Pfeifer, J. Caro, B. Zibrowius, M. Bulow, R. Mostowicz, Investigation of internal silanol groups as structural defects in ZSM-5-type zeolites, *Journal of the Chemical Society, Faraday Transactions 1: Physical Chemistry in Condensed Phases*, 83 (1987) 3459-3468.
- [45] Z. Wang, Y. Jiang, Y. Zhang, J. Shi, C. Stampfl, M. Hunger, J. Huang, Identification of Vicinal Silanols and Promotion of Their Formation on MCM-41 via Ultrasonic Assisted One-Step Room-Temperature Synthesis for Beckmann Rearrangement, *Industrial & Engineering Chemistry Research*, 57 (2018) 5550-5557.
- [46] A. Cauvel, D. Brunel, F. Di Renzo, E. Garrone, B. Fubini, Hydrophobic and Hydrophilic Behavior of Micelle-Templated Mesoporous Silica, *Langmuir*, 13 (1997) 2773-2778.
- [47] J.R. Martínez, F. Ruiz, Y.V. Vorobiev, F. Pérez-Robles, J. González-Hernández, Infrared spectroscopy analysis of the local atomic structure in silica prepared by sol-gel, *Journal of Chemical Physics*, 109 (1998) 7511-7514.
- [48] P. Innocenzi, Infrared spectroscopy of sol-gel derived silica-based films: a spectromicrostructure overview, *Journal of Non-Crystalline Solids*, 316 (2003) 309-319.
- [49] E.M. Björk, P. Mäkie, L. Rogström, A. Atakan, N. Schell, M. Odén, Formation of block-copolymer-templated mesoporous silica, *Journal of Colloid and Interface Science*, 521 (2018) 183-189.
- [50] J.S. Kim, R.H. Friend, F. Cacialli, Surface energy and polarity of treated indium-tin-oxide anodes for polymer light-emitting diodes studied by contact-angle measurements, *Journal of Applied Physics*, 86 (1999) 2774-2778.
- [51] J.-P. Dacquin, H.E. Cross, D.R. Brown, T. Duren, J.J. Williams, A.F. Lee, K. Wilson, Interdependent lateral interactions, hydrophobicity and acid strength and their influence on the catalytic activity of nanoporous sulfonic acid silicas, *Green Chemistry*, 12 (2010) 1383-1391.

Sol-gel synthesis of SBA-15: impact of HCl on surface chemistry

Cyril Pirez^{*a}, Jean-Charles Morin^a, Jinesh C. Manayil^b, Adam F. Lee^c and Karen Wilson^{*c}

^a UCSS, Université de Lille Nord de France, Lille, France

^b European Bioenergy Research Institute, Aston University, Birmingham, B4 7ET, UK

^c School of Science, RMIT University, Melbourne, Vic 3001, Australia

***Corresponding Authors:** karen.wilson2@rmit.edu.au; cyril.pirez@gmail.com

Highlights

- Impact of [HCl] on silanol distribution of sol-gel synthesised SBA-15 explored.
- Increasing [HCl] from 0.1 to 2.0 M doubles the surface silanol loading.
- Increased [HCl] favours hydrophilic geminal and vicinal silanols.
- SBA-15 surface energy and polarity correlates with [HCl] and surface silanols.